UNIVERSIDAD AUTÓNOMA DE BAJA CALIFORNIA

FACULTAD DE CIENCIAS MARINAS

INSTITUTO DE INVESTIGACIONES OCEANOLÓGICAS

MAESTRÍA EN CIENCIAS EN OCEANOGRAFÍA COSTERA

RESPUESTA DE LA CIRCULACIÓN SUBMAREAL EN UN ESTUARIO TROPICAL A LA COMPETENCIA DE DOS DESCARGAS FLUVIALES

TESIS

QUE PARA CUBRIR PARCIALMENTE LOS REQUISITOS NECESARIOS PARA OBTENER EL GRADO DE

MAESTRA EN CIENCIAS EN OCEANOGRAFÍA COSTERA

PRESENTA

ELISA VILLEGAS RODRÍGUEZ

Ensenada, Baja California, México

Octubre, 2025

FACULTAD DE CIENCIAS MARINAS

INSTITUTO DE INVESTIGACIONES OCEANOLÓGICAS

RESPUESTA DE LA CIRCULACIÓN SUBMAREAL EN UN ESTUARIO TROPICAL A LA COMPETENCIA DE DOS DESCARGAS FLUVIALES

TESIS

QUE PARA CUBRIR PARCIALMENTE LOS REQUISITOS NECESARIOS PARA

OBTENER EL GRADO DE

MAESTRA EN CIENCIAS EN OCEANOGRAFÍA COSTERA

Presenta

ELISA VILLEGAS RODRÍGUEZ

Aprobada por:

Dr. Braulio Juárez Araiza

Director de tesis

JOSE MAURO VARGAS HERNANDEZ (FIRMA)
PERSONA FISICA, CPF-02-0565-0871.
Fecha declarada: 27/10/2025 02:05:55 p. m.
Esta es una representación gráfica únicamente,
verifique la validez de la firma.

Dr. José Mauro Vargas Hernández

Sinodal

Dr. Arnoldo Valle Levinson

Sinodal

Dr. Isaac Rodríguez Padilla

Sinodal

Resumen

Comprender los impactos fluviales en la circulación estuarina es clave para proponer estrategias de gestión adecuadas para los ecosistemas estuarinos. La laguna Madre de Dios es un estuario tropical situado en la costa del Caribe de Costa Rica. El estuario recibe aportes de agua dulce de dos ríos, el río Pacuare, cercano a la boca, y el río Madre de Dios, situado cerca de la cabeza del estuario. Se llevaron a cabo dos campañas de mediciones para estudiar la respuesta de la circulación submareal bajo diferentes condiciones de descarga fluvial. La primera campaña se realizó del 7 de diciembre de 2017 al 16 de enero de 2018, y la segunda del 21 de marzo al 19 de abril de 2018. Se instalaron un perfilador acústico de corrientes Doppler (ADCP) y un sensor CTD (conductividad-temperatura-profundidad) en un canal a 1,5 km al sur de la boca del estuario. Los resultados mostraron que, en la primera campaña, el aumento del caudal del río Madre de Dios provocó un flujo submareal verticalmente homogéneo en dirección hacia el mar. Por el contrario, el río Pacuare indujo un flujo submareal superficial hacia la cabeza del estuario. Las inversiones en el flujo submareal observadas durante la segunda campaña se producen por el atrapamiento de agua salada introducida por la marea causado por una elevada descarga del río Pacuare, de manera que el agua salada atrapada forma una región de máxima salinidad. Esta máxima salinidad podría invertir los gradientes de densidad, lo que daría lugar a una circulación inversa hacia la boca, en concordancia con los datos observados de ADCP. En conjunto, estos hallazgos y los mecanismos propuestos evidencian que la circulación estuarina está dominada por el aporte fluvial y controlada por la interacción entre la hidrología y la morfología

Abstract

Understanding riverine impacts on estuarine circulation is key to propose adequate management strategies of estuarine ecosystems. Madre de Dios Lagoon is a tropical estuary located in the Costa Rica's Caribbean coast. It receives freshwater inputs from two rivers, the Pacuare river, adjacent to the inlet, and the Madre de Dios River, located toward the estuary's head. Two month-long campaigns were performed to study the circulation response to competing river-discharge conditions. The first campaign was from December 7th 2017 to January 16th 2018, and the second from March 21st to April 19th 2018. An Acoustic Doppler Current Profiler (ADCP) and a CTD (Conductivity-Temperature-Depth) sensor were moored in a channel at ~1.5 km landward (southward) of the inlet. Results showed that in the first campaign increased river-discharge from the Madre de Dios River forced a vertically homogeneous seaward flow in the channel. In contrast, the Pacuare River induced a surface landward flow. The observed flows during the second campaign consists of a tidally induced salinity intrusion that is trapped by an elevated Pacuare discharge; thus, salty water may become trapped, forming a localized region of maximum salinity. This salinity maximum could inverse density gradients yielding an inverse circulation near the inlet, as observed with the ADCP. These findings and the proposed mechanisms highlight the dominance of river-specific forcing in estuarine circulation and emphasize the interplay between hydrology and morphology

Tabla de contenido

AGRADECIMIENTOS

- A la Facultad de Ciencias Marinas y al Instituto de Investigaciones Oceanológicas de la Universidad Autónoma de Baja California por aceptarme en el programa de posgrado de maestría en ciencias en oceanografía costera.
- A la Secretaria de Ciencia, Humanidades, Tecnología e Innovación por la beca No. 1276586, que me dio la oportunidad de realizar este trabajo en los últimos dos años.
- A mi comité constituido por los doctores Braulio, Mauro, Isaac y Arnoldo, por su apoyo en la realización de este trabajo y por las enseñanzas de vida que me han brindado.
- A mi futura familia, quienes son el principal motivo para dar lo mejor de mí. Ser su madre es el sueño más grande que tengo y la razón por la que sigo avanzando aun cuando las fuerzas parecen no bastar.
- A mi núcleo familiar, que ha estado presente en cada momento. Mi madre Irma, mi padre Armando, mi abuela Lucy, mis hermanos Paloma, Esteban y Naomy, mi abuelo Gil, mi cuñado Rafael y mi sobrina Luna.
- A los que ya no están pero que me amaron y apoyaron, mi tío Guillermo (memo), mi abuela Esperanza (perita) y mi muy amada tía Tere (la hermanuana).
- A mis amistades del posgrado, conocerles me ha enseñado a vivir. No estaría aquí de no ser por sus ánimos en cada parte de este proceso.
- A mis amistades en general, gracias por acompañarme y escucharme hablar de mi trabajo y vida personal y por hacer lo posible por entenderme en ambos.
- A todas aquellas personas que sin saberlo han sido un pilar. A veces ofreciendo un hombro, a veces un oído, pero casi siempre mucho más que eso.
- A la iglesia, por ser un refugio para mí en tantas etapas y en tantas formas.

–

– 1ra de Tesalonicenses 5:18

Tabla de figuras

Capítulo 1. Los estuarios y su importancia

Introducción general

Los estuarios son cuerpos costeros semicerrados conectados al océano a través de una o más aperturas que reciben el aporte intermitente de agua dulce de uno o más ríos (Cameron and Pritchard 1963). Los estuarios pueden clasificarse bajo distintos criterios, como lo son su formación tectónica (Pritchard, 1952;1960) o su balance de aguas (Valle-Levinson, 2010).

Existen cuatro categorías que dependen de su formación tectónica: valles fluviales inundados, fiordos, estuarios tectónicos y estuarios de barra (Pritchard, 1960). La mayoría de los estuarios alrededor del mundo corresponden a la categoría de valles fluviales inundados (Perillo, 1995). Los estuarios de este tipo fueron formados por inundaciones de los valles fluviales a causa del aumento del nivel del mar durante la transgresión Flandriense (Pleistoceno-Holoceno) y se encuentran mayormente en latitudes bajas y medias (Perillo, 1995). Generalmente este tipo de estuarios muestran profundidades en su boca de ~25 m que disminuyen hacia la cabeza (Perillo, 1995; Pritchard, 1960). Los fiordos se encuentran en latitudes altas, donde las zonas montañosas estuvieron cubiertas de hielo durante el Pleistoceno. El hielo erosionó el fondo formando valles y su posterior retroceso produjo su inundación (Perillo, 1995; Pritchard, 1960). Los fiordos se caracterizan por tener canales profundos (200-800 m) y estrechos, con la presencia de un umbral asociado a la acumulación de material sedimentario depositados por actividad glaciar (Perillo, 1995). Los fiordos se subdividen en dos categorías con base en su actividad glaciar: fiordos rivereños y fiordos glaciales (Valle-Levinson, 2010). Los fiordos rivereños se asocian a glaciares extintos y su boyancia se debe principalmente al aporte fluvial, mientras que los fiordos glaciales están asociados a glaciares activos y su boyancia proviene del derretimiento glaciar (Valle-Levinson, 2010). Los estuarios de barra son formados cuando procesos litorales dominan sobre el rango de marea y el aporte fluvial, induciendo la formación de una barra arenosa, formando un cuerpo

costero semicerrado (Perillo, 1995; Valle-Levinson, 2010). Este tipo de estuarios suelen ser someros con profundidades promedio alrededor de 2 m. Los estuarios tectónicos, como su nombre lo indica, se forman por actividad tectónica, como movimientos en la corteza terrestre que provocan su hundimiento y generan una cuenca. Cuando esta cuenca es inundada por agua marina, se origina un estuario (Valle-Levinson, 2010).

La clasificación de estuarios con base en su balance de aguas tiene tres categorías: estuarios positivos, estuarios negativos, y estuarios de aporte reducido (Valle-Levinson, 2010). Los estuarios positivos son aquellos que reciben un aporte constante de agua dulce que genera una variabilidad longitudinal de densidad que incrementa de la cabeza hacia la boca (positivo). La circulación en los estuarios positivos consiste en agua saliendo del sistema por la superficie y agua de mar entrando al sistema por el fondo (Valle-Levinson, 2010). En los estuarios negativos, la variabulidad longitudinal de densidad se invierte creciendo de la boca a la cabeza del estuario generando un flujo de salida por el fondo y un flujo de entrada de agua proveniente del océano por la superficie (Pritchard, 1967; Valle-Levinson, 2022). Los estuarios de aporte reducido son aquellos donde la tasa de aporte fluvial es menor o de igual orden de magnitud que la perdida de agua (i.e. evaporación) (Largier et al., 1997).

El gradiente longitudinal de densidad representa la principal forzante de la circulación estuarina (Pritchard, 1967; Lange et al., 2020). Este gradiente es sensible a cambios estacionales en el estuario, pudiendo modificar temporalmente la circulación de positiva a negativa según la estación del año o del ciclo de mareas viva-muerta (Valle-Levinson & Schettini, 2016). La circulación estuarina también puede ser invertida de positiva a negativa por la presencia de eventos meteorológicos extremos, como vientos extremos o lluvias intensas (Lange et al., 2020). En el caso de los vientos, se ha documentado que las intensificaciones en los vientos hacia tierra pueden producir inversiones temporales en la circulación estuarina. Los vientos hacia el mar pueden intensificar la circulación y la estratificación

en un estuario positivo, mientras que los vientos hacia tierra pueden inhibir la circulación y estratificación (Scully et al. 2005). Por su parte, Chen y Sanford (2009) relacionaron el esfuerzo del viento y el gradiente longitudinal de densidad con un efecto de deformación por viento (*wind-straining*), demostrando mediante modelación numérica que la acción del viento hacia la cabeza del estuario reduce la estratificación en la columna de agua, mientras que la acción del viento en la boca puede fortalecer o debilitar la estratificación dependiendo de su magnitud

La circulación estuarina puede verse también modificada por eventos de lluvias intensas que aumentan el caudal de los ríos y que pueden modificar la intrusión mareal modificando la forzante principal en el estuario (Guerra-Chanis et al., 2021; Valle-Levinson, 2022). Por ejemplo, los pulsos de lluvia intensos durante huracanes pueden generar un flujo residual vaciante dominante y uniforme en la entrada del estuario (Guerra-Chanis et al., 2021). El flujo barotrópico asociado a la descarga de rio intensificada por lluvias puede dominar sobre la circulación estuarina típica y generar un cambio de un sistema dominado por mareas a un sistema dominado por el aporte fluvial (Guerra-Chanis et al., 2021). Este estudio proporciona un punto de referencia para comprender la posible respuesta del estuario a una fuerza hidrológica extrema.

El presente estudio es relevante dado que los estuarios son zonas de importancia ecológica y humana. Las zonas costeras tienen tasas de crecimiento más altas que las regiones tierra adentro (Neumann et al., 2015). Tres cuartas partes de las ciudades más pobladas del mundo están asentadas en estuarios o se ven influenciadas por ellos (Valle-Levinson, 2022, p. 1). El crecimiento demográfico y la urbanización repercuten en la calidad del agua de estas regiones, ejerciendo presión sobre los ecosistemas estuarinos y los recursos naturales debido al aumento del consumo de agua y la contaminación (Guo, 2022; Neumann et al., 2015). El crecimiento socioeconómico en las zonas cercanas a los sistemas estuarinos expone a las poblaciones al aumento del nivel del mar y a los efectos

relacionados con el cambio climático, lo que aumenta los niveles de riesgo y vulnerabilidad (Neumann et al., 2015). Además, los estuarios no solo fomentan actividades económicas como el turismo, el ocio y la educación (Wetz et al., 2013), sino que también proporcionan hábitats para una gran diversidad de especies. La gestión adecuada de las zonas estuarinas favorece la conservación de la flora fauna que dependen de ellas, dado que los estuarios proporcionan nichos para organismos con rangos específicos de tolerancia a la salinidad (Vasconcelos et al., 2024), así como áreas de alimentación para numerosas especies de aves migratorias durante todo el año (Botto et al., 1998). Comprender la hidrodinámica de los sistemas estuarinos beneficia a las comunidades circundantes al ayudar en la planificación y las estrategias de mitigación, como la restauración de humedales en zonas vulnerables al aumento del nivel del mar (Temmerman et al., 2013).

Capítulo 2. Artículo sometido. Estuarine Coastal and Shelf Science

Flow Responses in a Tropical Estuary to a Pair of Competing River Discharges

[a,b] Villegas-Rodríguez Elisa, [b] Juárez Braulio, [c] Vargas-Hernández J. Mauro, [d] Valle-Levinson Arnoldo, [b] Rodríguez P. Isaac

[a] *Facultad de Ciencias Marinas, Universidad Autónoma de Baja California, Ensenada, México*

[b] *Instituto de Investigaciones Oceanológicas, Universidad Autónoma de Baja California, Ensenada, México*

[c] *Laboratorio de Oceanografía y Manejo Costero, Departamento de Física, Universidad Nacional, Heredia, 86-3000, Costa Rica*

[d] *Department of Civil and Coastal Engineering, University of Florida, Gainesville, FL 32611, USA*

Abstract

Understanding riverine impacts on estuarine circulation is key to propose adequate management strategies of estuarine ecosystems. Madre de Dios Lagoon is a tropical estuary located in the Costa Rica's Caribbean coast. It receives freshwater inputs from two rivers, the Pacuare river, adjacent to the inlet, and the Madre de Dios River, located toward the estuary's head. Two month-long campaigns were performed to study the circulation response to competing river-discharge conditions. The first campaign was from December 7th 2017 to January 16th 2018, and the second from March 21st to April 19th 2018. An Acoustic Doppler Current Profiler (ADCP) and a CTD (Conductivity-Temperature-Depth) sensor were moored in a channel at ~1.5 km landward (southward) of the inlet. Results showed that in the first campaign increased river-discharge from the Madre de Dios River forced a vertically homogeneous seaward flow in the channel. In contrast, the Pacuare River induced a surface landward flow. The observed flows during the second campaign consists of a tidally induced salinity intrusion that is trapped by an elevated Pacuare discharge; thus, salty water may become trapped, forming a localized region of maximum salinity. This salinity maximum could inverse density gradients yielding an inverse circulation near the inlet, as observed with the ADCP. These findings highlight the dominance of river-specific forcing in estuarine circulation. The proposed mechanisms underscore the interplay between hydrology and morphology.

Keywords: Estuary, density gradient, subtidal flow, river-induced

1. Introduction

Estuaries are traditionally defined as semi-enclosed coastal bodies connected to the ocean through one or more inlets and receive internment freshwater inputs from one or more rivers (Cameron and Pritchard 1963). Estuaries are classified in three groups based on their water balance: positive, negative, and low-inflow estuaries (Valle-Levinson, 2010). Positive estuaries are defined by freshwater gains, driving a longitudinal density gradient that increases seaward and promotes a surface freshwater outflow and a seawater inflow underneath (Valle-Levinson, 2010). These patterns reverse in negative estuaries due to net freshwater losses (Pritchard, 1967; Valle-Levinson, 2022). Low-inflow estuaries are those where freshwater input rates are smaller or of the same magnitude order as water losses (i.e. evaporation) (Largier et al., 1997).

In estuarine systems, the longitudinal density gradient is the major driver of the estuarine circulation; also referred as gravitational flow (Pritchard, 1967; Lange, et al., 2020). The reversal of gravitational circulation can be triggered by extreme meteorological events, such as heavy rainfall or winds (Lange, et al., 2020). These events can also modify the length of tidal intrusion, potentially altering the estuary's dominant forcing (Guerra-Chanis et al., 2021; Valle-Levinson, 2022). The density gradient modulates subtidal circulation and exhibits sensitivity to seasonal changes, temporarily shifting an estuary from positive to negative over seasonal or from spring to neap tides (Valle-Levinson & Schettini, 2016).

Extreme rainfall pulses are capable of inducing temporary alterations in estuarine circulation. The impact of such events is exemplified by the case study of Hurricane Irma on the Suwannee River estuary (Guerra-Chanis et al., 2021). Their research revealed that the hurricane's precipitation generated a dominant, depth-uniform seaward flow that persisted throughout the entire water column after the storm passage. This barotropic flow structure effectively supplanted the typical estuarine two-layer circulation, highlighting a shift from a tidally modulated system to a fluvial-dominated regime. The findings of Guerra-Chanis et al. (2021) thus underscore the power of precipitation events to overwhelm tidal forcing and establish fluvial-dominated seaward flow conditions. Such case study provides a reference point for understanding the potential estuarine response to extreme hydrological forcing.

This study aims to understand the subtidal circulation response in a tropical estuary under different meteorological scenarios using ADCP-derived subtidal current profiles. This objective is addressed by correlating the observed flow patterns with meteorological parameters.

1.2 Study Area

Madre de Dios Lagoon is a tropical estuary in the Costa Rica's Caribbean coast at latitude 10.22° N (figure 1). It receives freshwater inputs from two rivers, the Pacuare river, adjacent to the inlet (10.22° N), and the Madre de Dios River, located near the estuary's head (10.19° N). The distance from the Pacuare to the Madre de Dios River is 3.4 km; the Pacuare River is analogous to other rivers in the region (Lind, 2016), it source is in the Talamanca Mountains where the drier season is from January to April and the wetter period from May to December (Lind, 2016). The drainage area of the Pacuare river is 914 km^2, with a main channel length of 134.39 km, and an average rainfall up to 5000 mm y^{-1} (Picado & Umaña, 2018). The Madre de Dios River watershed covers ~240 km^2, is located at the province of Limon and is home to a diversity of species (Viéytez et al., 1983; Rämö et al., 2018). Its source is in the Caribbean in the Caribbean region, where maximum rainfall occurs from June to August and from December to February, in March-April and September-October occurs the less intense precipitations (Orozco-Montoya,& Penalba, 2023). Fifty-two percent of its area is used for farming bananas, pineapples, and rice, implying that the species inhabiting the estuary are exposed to pesticides (Echeverría-Sáenz et al., 2018). There is a lack of information regarding the system circulation and hydrography adding to the relevance of this study for the Costa Rica Caribbean region.

2. Methods

2.2 Data collection

Temperature, salinity, water pressure, and current data were collected at the main channel of Laguna Madre de Dios estuary by the Laboratorio de Oceanografía y Manejo Costero of the Department of Physics at Universidad National in Costa Rica during two field campaigns. The first campaign lasted 47 days, from December 7th, 2017 to January 16th, 2018. The second campaign lasted 29 days, from March 21st to April 19th, 2018. Water level and current data were obtained using an Acoustic Doppler Current Profiler (ADCP) moored at 5.3 m depth at coordinates 10.21421°N and 83.2751°W (Fig. 1). The ADCP measured at sampling intervals of 15 minutes for

the first campaign and 10 minutes for the second campaign. Both surveys used vertical cells of 0.5 m size, with the first cell located 1.5 m above the bottom. Salinity and temperature data were collected with a CTD anchored alongside the ADCP, using the same sampling intervals.

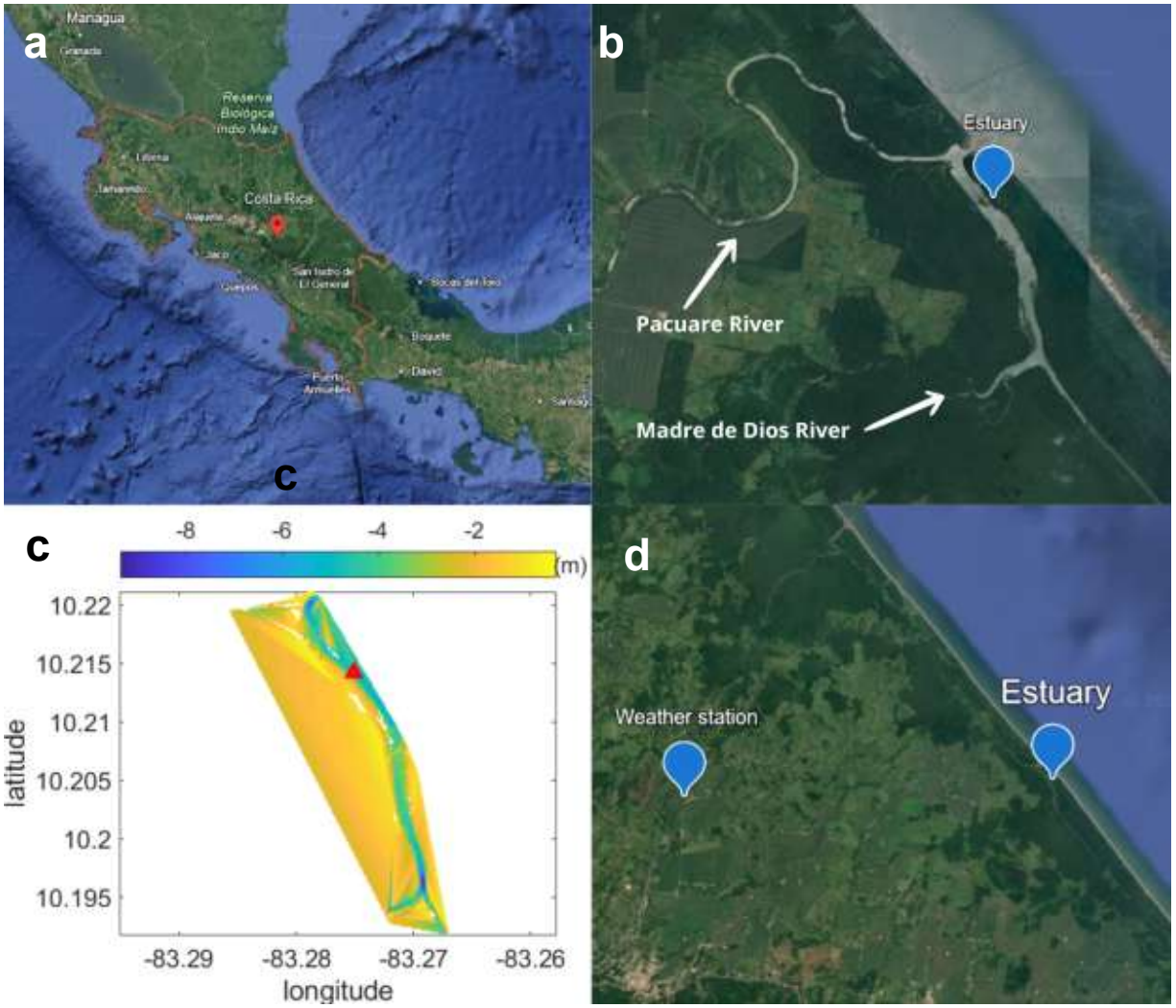

Figure 1. a) Costa Rica. b) Madre de Dios Lagoon Estuary, Pacuare river, Madre de Dios river and instrument location. c) ADCP and CTD mooring location (red triangle) in the estuary bathymetry. d) Meteorological station location.

2.3 Data analysis

The amplitudes of the principal tidal constituents were first determined by applying harmonic analysis through least-squares fit (Weisstein, 2002; Li, 2022) to the current velocity data to classify

the tidal regime. The main constituents used in the least-squares fit were the components S2 (12 h), M2 (12.42 h), N2 (12.66 h), K1 (23.93 h), O1 (25.82 h). The amplitudes obtained by harmonic fit were used to calculate the tidal form factor, defined as $F = (K_1 + O_1) / (M_2 + S_2)$. A value of $F = 0.89$ indicates a mixed- semidiurnal tidal regime. Velocity data were projected stream-wise. A 30-hour cutoff Lanczos low-pass filter removed tidal frequencies from the time series of currents, temperature, and salinity. The Lanczos filter used a smoothed cutoff, minimizing signal distortions associated with the Gibbs phenomenon (Thomson & Emery, 2014). A principal component analysis (Abdi and Williams, 2010) identified the dominant patterns of temporal and spatial variability in the stream-wise component of the velocity profiles during the campaigns. The accumulated rainfall for both field campaigns was calculated from hourly meteorological data from a wheatear station 22 km away from the estuary, provided by the National Meteorological Institute of Costa Rica (IMN).

2.4 Theoretical Density Gradient Estimation

Additionally, a least-squares fit was applied to the profile of filtered (subtidal) velocity using an analytical model proposed by Valle-Levinson et al. (2019) to obtain a theoretical horizontal density gradient scaled by the vertical eddy viscosity. In their work, Valle-Levinson et al. (2019) defined the governing dynamics as linear, quasi-stationary, non-rotational, and laterally invariant. The momentum balance was given by:

$$Az\frac{\partial^2 \mathrm{u}}{\partial z^2} = g\frac{\partial \eta}{\partial x} + \frac{g}{\rho 0}\frac{\partial \rho}{\partial x}H$$

where Az is vertical eddy viscosity (0.001 $m^2\ s^{-1}$); z is the vertical coordinate (m); H is total water column depth (m); g is gravitational acceleration (m s^{-2}); ρ is a reference density (1020 kg m^{-3}); $\partial\rho/\partial x$ is the longitudinal density gradient (kg m^{-4}); $\partial\eta/\partial x$ is the subtidal water-level slope. The solution to the equation as a function of depth is solved by integrating twice respect to z, taking as boundary condition no-slip at the bottom ($u = 0$ at $z = -H$) and wind stress acting on the surface, $\partial u/\partial z = \tau/(\rho Az)$ at $z = 0$, (Valle-Levinson *et al.*, 2019; Valle-Levinson, 2022). To express the water-level slope in terms of the horizontal density gradient, Valle-Levinson et al. (2019) set the condition that the vertical average of the velocity equals ua. The solution to the equation becomes:

$$u(z) = \frac{3}{2}ua\left[1 - \frac{z^2}{H^2}\right] - \frac{gH^3}{48\rho}\frac{\partial\rho}{\partial x}\frac{}{Az}\left[9\left(1 - \frac{z^2}{H^2}\right) - 8\left(1 + \frac{z^3}{H^3}\right)\right] + \frac{H}{4\rho}\frac{\tau}{Az}\left[4\left(1 + \frac{z}{H}\right) - 3\left(1 - \frac{z^2}{H^2}\right)\right]$$

where *ua* is the depth averaged flow (m s^{-1}); τ is the wind stress (pa). The first term of the model represents the barotropic flow related to the river freshwater pulses (Valle-Levinson et al., 2019). The second term of the model represents subtidal flow forced by longitudinal density gradients. The magnitude of this forcing is sensitive to water depth and depends on the ratio between the horizontal density gradient and turbulent viscosity coefficient (Valle-Levinson et al., 2019). The third term represents the subtidal wind-driven flow related to the wind stress and the vertical eddy viscosity ($\frac{\tau}{Az}$) (Valle-Levinson et al., 2019).

3 Results

Results from both campaigns are described in chronological order. The first campaign occurs during the Caribbean rainiest period of the year from December 2017 to January 2018. Data collected during the second campaign, from March to April 2018, covers a period of less intense rainfall than the first campaign.

3.2 First campaign from December 2017 to January 2018.

The time series began with a peak in subtidal water level on December 10th produced by a rainfall pulse that started on December 8th and reached an accumulated rainfall of 54 mm (Fig. 2 upper and second panel). The pulse of freshwater yielded a homogenous outflow of freshwater denoted by the decrease in temperature and zero salinity that showed a sporadic increase by December 18th when the subtidal water level displayed negative values. This temperature and salinity values evidenced a dominance of riverine input over marine influence. From December 10th to December 17th a period of constant reduced rainfall occurred, ~20 mm. Around the second spring tide, subtidal salinity displayed double-peak pattern with the maximum salinity, ~14 g/kg, displayed on December 30th. The salinity increase was interrupted by a second rainfall that began

around January 2nd and coincided with a positive subtidal water level. Accumulated rainfall increased up to ~400 mm, that represented an accumulation of approximately 149 mm in five days up to December 7th when subtidal water level peaked to 0.3 m. This rainfall pulse must trigger a river pulse that decreased salinity from 10 g kg^{-1} to freshwater conditions (0 g kg^{-1}). Both events exhibited similar temporal drops in salinity and suggests a relationship between rainfall pulses with the Madre de Dios River freshwater input.

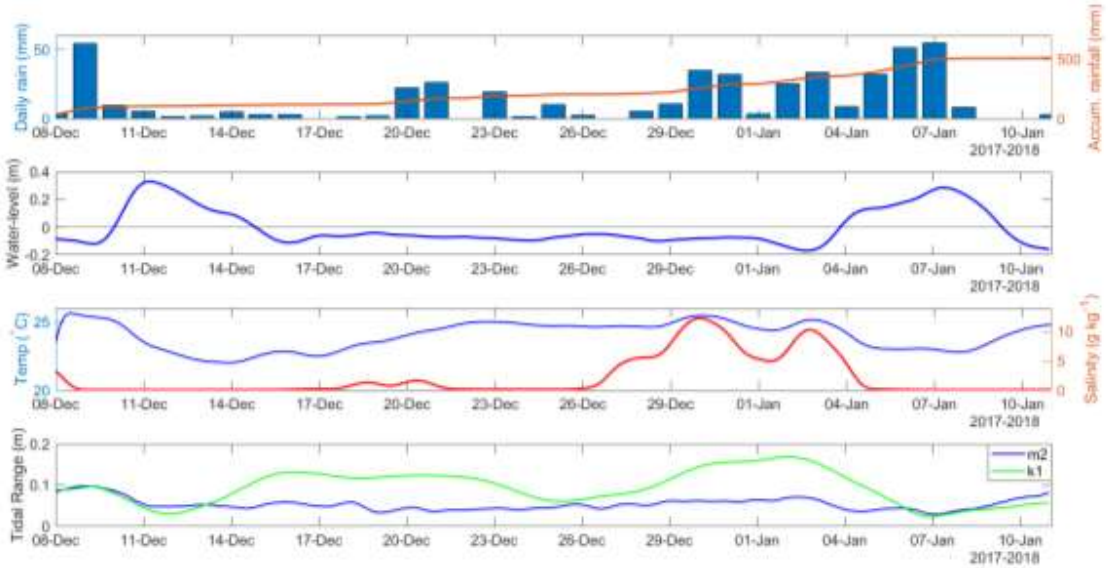

Figure 2. Time series of accumulated rainfall (mm, upper panel), subtidal water level (m, second panel), and temperature (°C, third panel, blue line) and salinity (g kg-1, third panel, red line), tidal range (m, lower panel). Tidal range of the tidal component M2 (blue line) and K1 (green line), (lower panel).

The subtidal along-channel velocity profile was dominated by a persistent, and vertically-homogeneous seaward flow pattern (Fig. 3, upper panel) distinguished by two seaward flow pulses. The first pulse of ~11 cm s^{-1} was triggered by the rainfall event around December 11th, described above. During this event, the seaward pulse generated a subtidal water-level increase. The pulse lasted until December 13th and was followed by negative water levels. From December 14th until early January, the seaward flow depicted subtidal velocities of 5 cm s^{-1}. The second

pulse consisted of maximum seaward currents of 20 cm s^{-1}, the highest velocities recorded during the deployment.

The statistical significance and dominance of this riverine-driven flow was confirmed through principal component analysis (PCA). The first principal component explained 97% of the total variance of the subtidal current signal (Fig. 3, upper panel). The spatial distribution of the first principal component consisted of a homogenous vertical profile (Fig. 4). The temporal variability of this mode coincides with the temporal variability of subtidal water-level (Figure 2, second panel). A cross-correlation analysis assessed a quantitatively and statistically significant (95% confidence level) correlation coefficient of 72% with a lag of 10.25 hours between the temporal evolution of principal component 1 and subtidal water-level fluctuations within the estuary. This correlation provides quantitative evidence that this first mode of circulation is related to discharge pulse events produced by accumulated rainfall. Thus, the temporal evolution and intensity of subtidal circulation were governed by the discharge of the river near the head, that depends of the Caribbean rainfall variability.

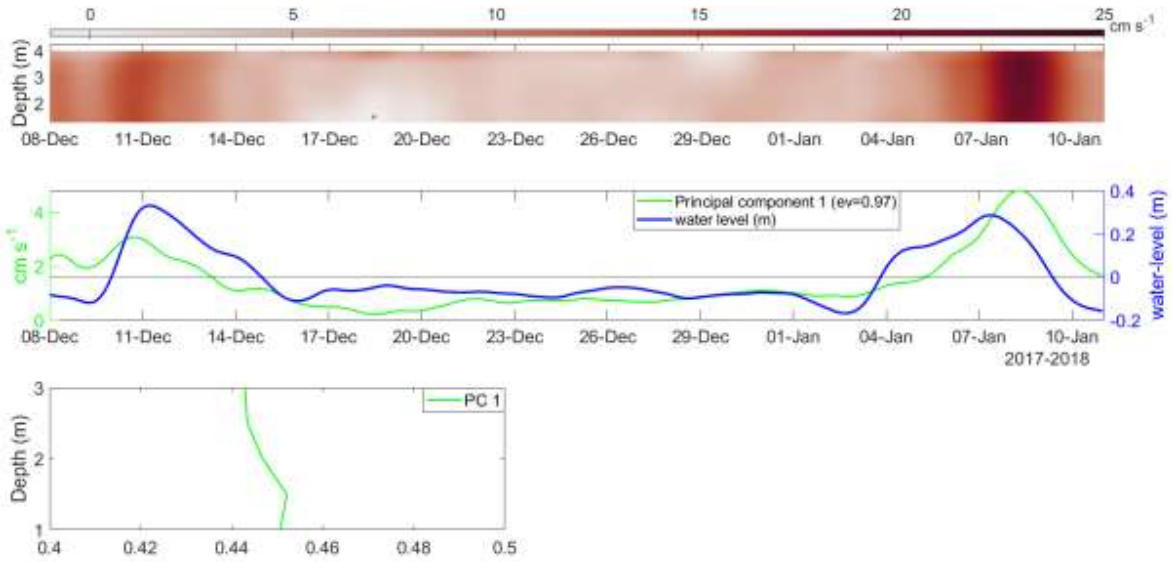

Figure 3. Time series of subtidal current velocities profile (upper panel); positive values represent outflow (seaward flow) and negative values indicate inflow (landward flow). Middle panel: temporal variability of first principal component obtained by the principal component analysis

(green line) and subtidal water level (blue line). Lower panel: spatial distribution of the first principal component of the first campaign.

3.3 Second Campaign (March to April 2018)

The time series of the second campaign started after a rainfall pulse event with an initial accumulation of approximately 40 mm (Fig. 4, upper panel). This rainfall pulse produced an increase in river discharge and induce a positive subtidal water-level increase of up to 0.1 m as observed on March 25th (Fig. 4, second panel). The hydrographic variables responded to the background conditions imposed by the rainfall and tide. Subtidal salinity and temperature decreased from 24 g kg^{-1} to 16 g kg^{-1}, and from 28°C to 27°C, respectively. A second rainfall pulse of ~10 mm on March 29th, caused a salinity decrease from 27 g kg^{-1} to 21 g kg^{-1} on April 1st. Notably, the water temperature, unaffected by the freshwater input, increased up to 28.6°C on April 4th. From April 2nd to 10th, subtidal water-level maintained negative values. A gradual salinity and temperature decrease is observed from April 4th to the end of the campaign. Subtidal water level values reversed from negative to positive on April 10th. In the final stage of the campaign, a period of constant rain, ~10 mm, triggered a temperature and salinity decrease.

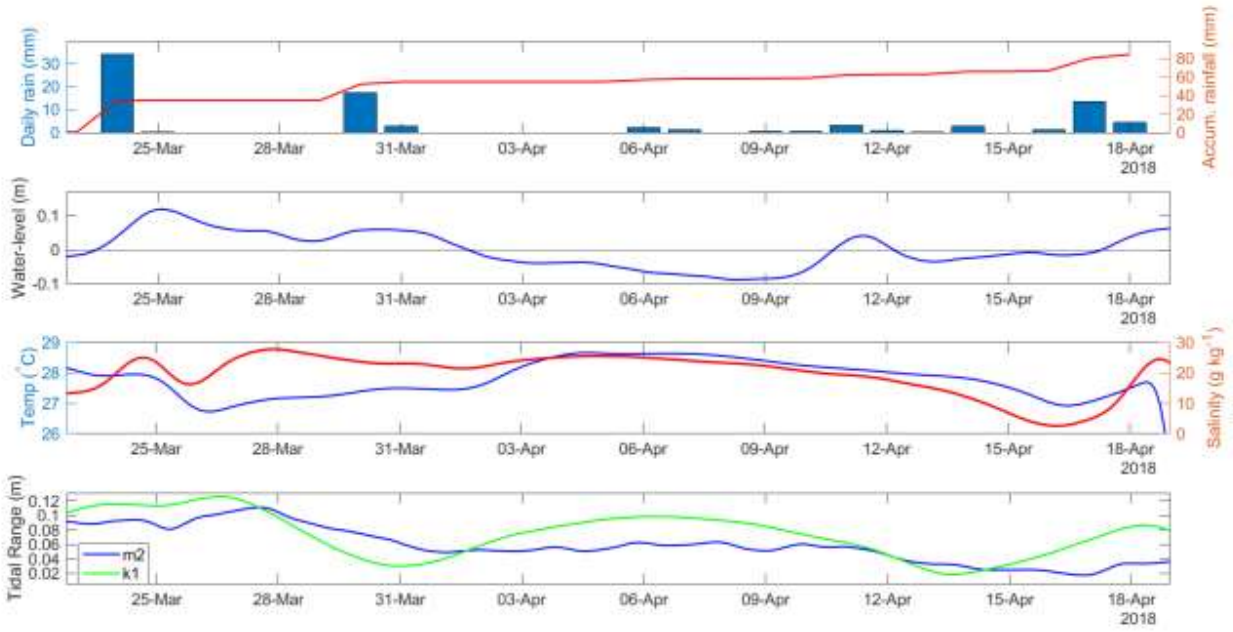

Figure 4. Accumulated rainfall (upper panel), non-tidal water level (second panel), and both temperature (third panel, blue line) and salinity (third panel, red line) data collected during the study period. Tidal range of the tidal components M2 (blue line) and K1 (green line), (fourth panel).

A vertically sheared subtidal flow profile was observed during the first recorded days; reminiscent of a classic two-layer estuarine circulation with inflows of ~1 cm s^{-1} and outflows of cm s^{-1} (Fig. 5, upper panel) The estuarine circulation shifted to a homogenous seaward flow with velocities of ~6 cm s^{-1} until March 27th. The homogeneous seaward flow was interrupted by a second estuarine circulation profile pattern, denoting a return flow-driven by gravitational forcing. From March 29th to April 6th, the two-layers circulation shifted to a homogeneous subtidal flow profile with velocities up to 3 cm s^{-1}. Around April 9th, the subtidal velocity profile displayed a two-layer vertical circulation, with inflows at the surface and outflows underneath reminiscent of an inverse estuarine circulation, with inflows of ~1 cm s^{-1}, and outflows of ~1 cm s^{-1}. This flow reversal persisted until April 10th when the profile shifted to a positive circulation two-layer mode. A second inverse estuarine circulation appeared from April 13th to 15th. The series ended on April 18th with a positive estuarine circulation.

The first principal component (Fig. 5, middle panel) accounted for 79% of the total variance in the time series. The temporal evolution of the first component demonstrated a relationship with the rainfall event, and the increase in subtidal water-level observed on March 25th. The correlation between the first principal component and the water-level was 67% with a lag of 10.22 hours with a confidence level of 95%, confirming the relationship within the first principal component and barotropic forcing mechanisms. The total variance explained by this component underscores the influence of river discharge on the subtidal circulation profiles during the study period. The spatial distribution of the first principal component displayed a homogeneous vertical variability throughout the water column (Fig. 6). The second principal component accounted for 19.9% of the total variance of the subtidal circulation (blue line in Fig. 5, lower panel). The spatial distribution of the second principal component showed a two-layer vertical circulation. The temporal variability of this mode exhibited a correspondence with the theoretical density gradient obtained from the analytical solution (Eq 1. Valle-Levinson et al, 2019). The cross-correlation between the second principal component and the modeled density gradient was 65% with a lag of 18.16 hours and a confidence level of 95%. This correlation value suggests that while the baroclinic forcing associated with the density gradient is a primary driver of principal component 2, it is not the sole contributor. The residual variance is likely attributable to other co-varying physical processes, such as remote wind stress, lateral advection, or non-linear tidal interactions, which were not directly quantified in this study but are known to modulate estuarine circulation (Pritchard, 1967; Lange, 2020; Valle-Levinson, 2010).

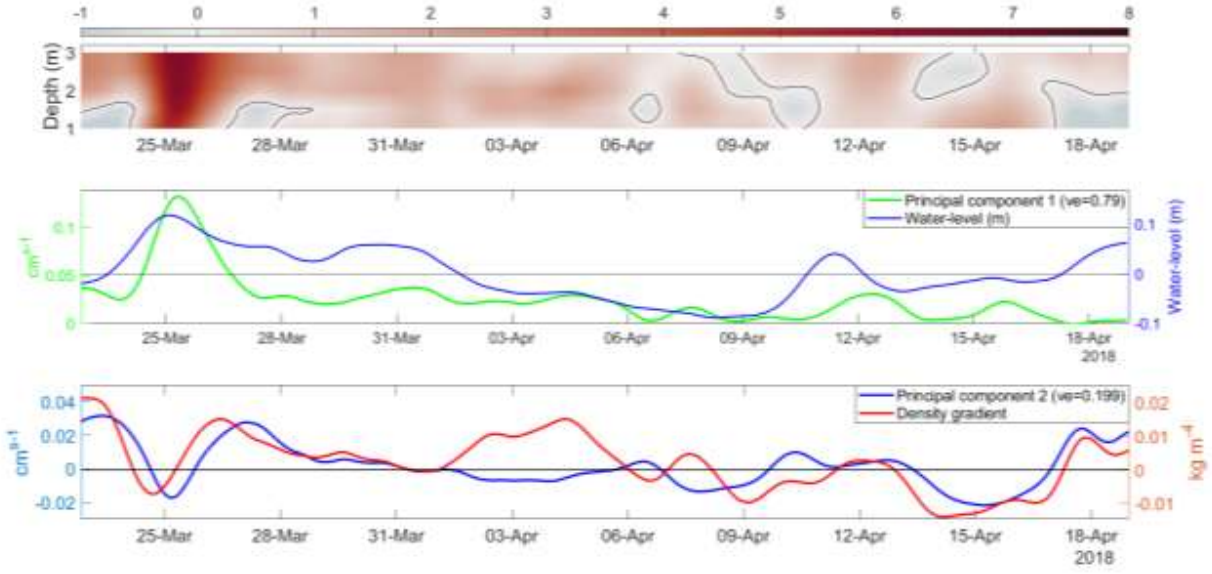

Figure 5. Time series of subtidal current velocities profile (upper panel); where positive values represent outflow from the estuary (seaward flow) and negative values indicate inflow (landward flow). First principal component (green line) and subtidal water level (blue line), (middle panel). Second principal component (bottom panel, blue line) with the theoretical density gradient (red line).

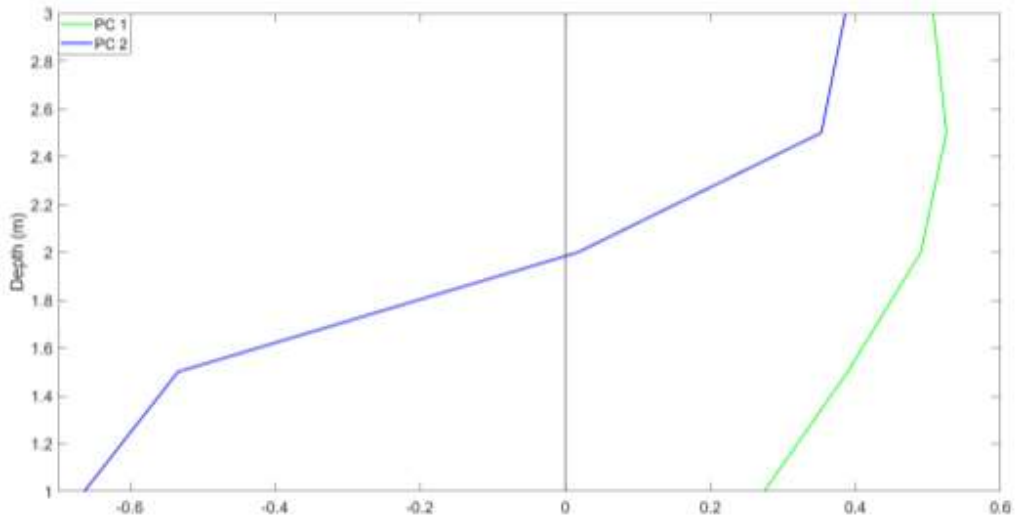

Figure 6. Spatial distribution of principal component 1 (green line) and 2 (blue line) of the second campaign.

4 Discussion

4.2 Circulation responses in a two-river system

During the first campaign, the region experienced persistent rainfall (Fig. 2, upper panel). The freshwater pulse from the river near the head of the estuary, driven by the rainfall rises, generated a sustained seaward freshwater flow throughout the entire time series (Fig. 7a and Fig. 3, upper panel). The observed flow from the first campaign aligns with other studies that documented the effects of high precipitation events on subtidal circulation and salinity patterns that reorganize estuarine circulation (Guerra-Chanis et al, 2021). During this campaign a depth-uniform seaward freshwater flow dominated the water column, representing a hydrological response to sustained precipitation in the watershed. This fluvial-driven regime was disrupted by episodes of saline intrusion induced by spring tidal incursion. The temporal variability of the circulation and the intermittent salinity intrusions underscores the dynamic nature of the circulation regimes in tropical estuaries subject to pulsed hydrological forcing. The rainfall-induced outflow indicated the dominance of the input from the river near the head in regulating subtidal circulation during the first study period.

The Pacuare River watershed covers Costa Rica's Central Valley region, a hydrological watershed characterized by its own precipitation regimes that contrasts with the Caribbean (Solano and Villalobos, IMN). Consequently, its discharge responds to localized rainfall patterns associated with the seasonal variability of the Central slope of Costa Rica and independent of those influencing the Madre de Dios River, which drains a separate watershed. This difference in the hydrological regimes sets a study case of individual river impacts on the estuary. The effects of the Pacuare's discharge were observed during the second half of the 2018 campaign when two episodes of inverse estuarine circulation occurred. During the second campaign the principal component 2 accurately reproduced the observed reversals in subtidal circulation and the estimated density gradient. The correlation between the principal component 2 and the estimated density gradient indicates that the reversals were driven by the density gradients.

4.3 Flow reversals due to a bifurcated river flow

The reversal of the estuarine circulation is linked to freshwater pulses from the river located near the head that modify the density gradients. The density differential between freshwater and seawater establishes a baroclinic pressure gradient. In this framework, less dense riverine water generates a surface outflow, as described by Valle-Levinson (2011, p. 75-86). In the studied system, a sudden increase in discharge from the river near the mouth generates a strong backwater effect. This effect manifests as a negative water-level slope propagating toward the estuary head, which subsequently modifies the established gradient and can induce a transient landward surface inflow. The magnitude of this water-level slope alteration and the resulting backwater effect would be intensified as the volume of freshwater discharge increases (Cai et al., 2016). This theoretical framework is further supported by observations in other estuarine systems worldwide (Cai et al., 2016; Saha & Cho, 2016). For instance, studies in the estuaries of Bangladesh by Saha & Cho (2016) provide quantitative validation of this physical principle, showing similar circulation reversals driven by remote freshwater inputs. Under this scenario, saline water imported during spring flood tides may become trapped within the estuary by a peak discharge from the river near the mouth of the estuary; leading to the formation of a region of maximum salinity (brackish salt-plug) within the estuary (Fig. 7, b), (i.e. Juarez et al, 2020). This phenomenon would generate a positive density gradient landward and a negative gradient seaward (Saha & Cho, 2016; Taleb et al., 2023). This density structure would restrict the connection between the upper estuarine reaches and coastal waters; while the downstream region continues to exchange freely with the Caribbean Sea (Saha & Cho, 2016). Under this hypothesized scenario, a weakening of the subtidal flow within the maximum salinity zone and a state of practically absent stratification are anticipated (Taleb et al., 2023).

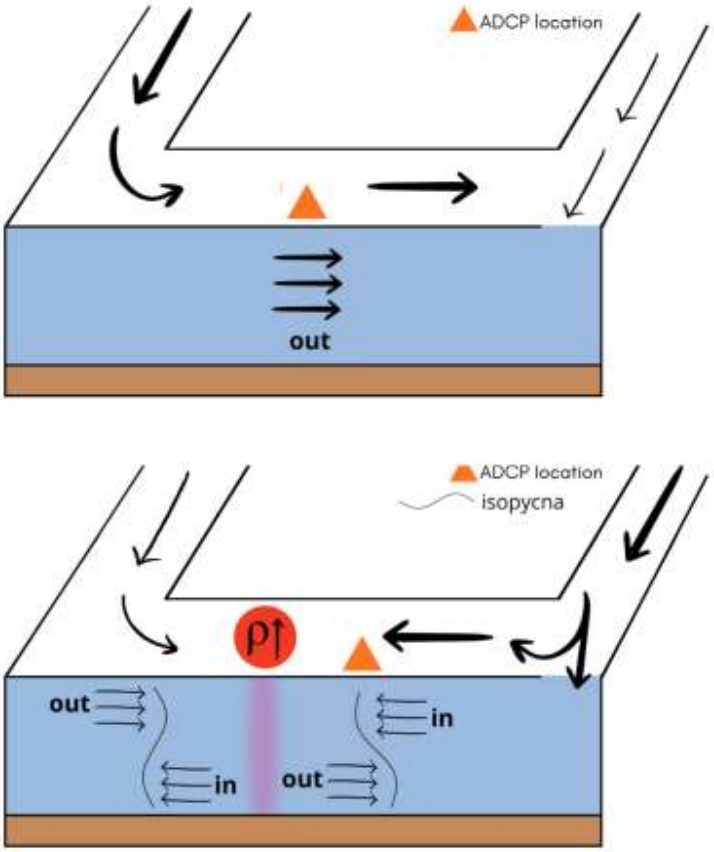

Figure 7. Sketch of the two circulation regimes presented for systems with the input of two rivers as in Madre de Dios estuary. a) Dominance of the river by the head: the increase in the discharge of the river near the head generates a sustained seaward freshwater outflow through the water column. b) Dominance of the river near the mouth: the increase in the discharge of the river near the mouth traps the seawater (red circle in b) that intrudes during flood tides, yielding to a maximum salinity (density) region that reverses the density gradient towards the estuary mouth, and triggers a negative estuarine circulation. The orange triangle denotes the ADCP location.

4.4 Study limitations

While this study provides insights into the forcing mechanisms within an estuary influenced by two river inputs, some limitations should be acknowledged. The observations are based on a single ADCP and CTD mooring that limits our conclusions to a restricted along- and a cross-channel location. A secondary current profiler instrument located in the channel shoal might shed light on the transversal structure of the subtidal circulation during the two case scenarios presented. Also, an

additional CTD located near the estuary inlet would facilitate the description of subtidal water-level slopes and density gradients to confirm the hypothesis suggested in Fig. 7 (bellow). Although the PCA analysis strongly links flow variability to water-level, and theoretical density-gradient changes, the influence of other factors such as wind forcing was neglected and could be incorporated into more comprehensive models in the future. These limitations highlight avenues for further research, such as deploying along- and cross-estuary arrays of sensors to capture spatial gradients and extending the monitoring period.

5 Conclusions

This study reveals two different subtidal circulation responses driven by the spatial location of two rivers that drain into the estuary. The first response occurred during increased discharge from a river located near the estuary's head (Madre de Dios River). The subtidal circulation response to the river pulse consisted of a vertically-homogeneous seaward flow, establishing freshwater conditions throughout the duration of the event. The second event triggered an inverse subtidal circulation associated with increased flow from the river adjacent to the estuary mouth (Pacuare River). The Pacuare river flow bifurcated with a seaward flow and a landward flow. We propose that the brackish landward flow traps oceanic salinity transported by flood tides, forming a brackish salt-plug. This salt-plug modifies the density gradient thereby reversing the observed inverse subtidal circulation. These findings highlight the critical role of freshwater input location in determining estuarine circulation.

Declaration of generative AI and AI-assisted technologies in the writing process

During the preparation of this work the author Villegas-Rodríguez used DeepSeek in the writing process to improve the readability and language of the manuscript. After using this tool/service, she reviewed and edited the content as needed and take full responsibility for the content of the published article.

Capítulo 3. Conclusiones generales

La circulación submareal de un estuario tropical se modificó en respuesta al aporte fluvial de dos ríos y estos cambios ocurrieron en función de la ubicación de cada uno de ellos. Los resultados revelan dos respuestas contrastantes bajo diferentes escenarios. Cuando el río dominante se encuentra en la cabeza del estuario, se genera un flujo hacia el mar verticalmente homogéneo en la columna de agua. Por el contrario, la intensificación del aporte de agua procedente del río adyacente a la boca provoca la bifurcación del pulso fluvial creando un flujo en dirección hacia la cabeza del estuario que genera un atrapamiento del agua salada previamente aportada por la marea. En este proceso se forma un tapón salino que invierte el gradiente longitudinal de densidad cambiando la circulación submareal de positiva a negativa.

Referencias

Abdi, H. and Williams, L.J. (2010), Principal component analysis. WIREs Comp Stat, 2: 433-459. https://doi.org/10.1002/wics.101

Botto F., Iribarne O., Martínez, M. (1998). *The effect of migratory shorebirds on the benthic species of three southwestern atlantic argentinean estuaries*. Estuaries, Vol 21, no.4B, p. 700-709

Cai H., Savenije H., Jiang C., Zhao L., Yang Q. (2016). Analytical approach for determining the mean water level profile in an estuary with substantial fresh water discharge. Hydrol. Earth Syst. Sci., 20, 1177–1195

Chen, S.-N., & Sanford, L. P. (2009). Axial wind effects on stratification and longitudinal salt transport in an idealized, partially mixed estuary. Journal of Physical Oceanography, 39, 1905–1920. https://doi.org/10.1175/2009JPO4016.1

Li, Chunyan. (2022). Generic Least Squares Method and Orthogonal Functions. *Time Series Data Analysis in Oceanography*. 178-189 pp. Cambridge

Dinesh C., Yang-Ki C. (2016). Sal Plug Formation Cuased by Decreased River Discharge in a Multi-Channel Estuary. Sientific Reports. 10.1038

Emery, W. J., & Thomson, R. E. (2014). Digital filters. In *Data analysis methods in physical oceanography* (3ra ed., pp. 539–584). Elsevier.

Echeverría-Sáenz, S., Mena, F., Arias-Andrés, M., Vargas S., Ruepert C., Van den Brink., Castillo L. (2018). In situ toxicity and ecological risk assessment of agro-pesticide runoff in the *Madre de Dios* River in Costa Rica. *Environ Sci Pollut Res* 25, 13270–13282

Guerra-Chanis, G., So, S., Valle-Levinson, A. (2021). *Effects of Hurricane Irma on residual flows and saltwater intrusion in a subtropical estuary*. Regional Studies In Marine Science, vol. *41*, DOI 10.1568

Guo Y. (2022). *Hydrodynamics in Estuaries and Coast: Analysis and Modeling*. Water. Vol 14, no. 9: 1478, DOI 10.3390

Lange, X., Klingbeil, K., & Burchard, H. (2020). Inversions of estuarine circulation are frequent in a weakly tidal estuary with variable wind forcing and seaward salinity fluctuations. Journal of Geophysical Research: Oceans, 125, e2019JC015789. https://doi.org/10.1029/2019JC015789

Largier J., Hollibaugh J., Smith S. (1997). Seasonally Hypersaline Estuaries in Mediterranean-climate Region. Esturine, Coastal and Shelf Science, 45, 789-797

Lind, P. (2016). Geomorphology and Sediments Dynamics of a Humid Tropical Montane River, Rio Pacuare, Costa Rica. [Doctoral dissertation, University of Oregon]. ProQuest Dissertations & Theses. 10194976

MATLAB. (2010). *version 7.10.0 (R2010a)*. Natick, Massachusetts: The MathWorks Inc.

Neumann, B. Vafeidis, A.T, Zimmermann, J. Nicholls, R.J. (2015). Future Coastal Population Growth and Exposure to Sea-Level Rise and Coastal Flooding—A Global Assessment. PLoS ONE, 10, e0118571

Orozco-Montoya, R.A., Penalba, O.C. Spatial and temporal rainfall variability in the Caribbean coast of Costa Rica. Theor Appl Climatol 151, 1585–1599 (2023). https://doi.org/10.1007/s00704-022-04342-8

Picado J., Umaña G. (2018). Fish assemblages and their ecological traits along an elevational gradient in the Rio Pacuare, Costa Rica. Revista de Biologia Tropical. Vol. 66 No.S1

Pritchard D.W. (1952). Salinity Distribution and Circulation in the Chesapeake Bay estuarine system. J. Mar. Res., 11:106-123

Pritchard D.W. (1962). Lectures on estuarine oceanography. B. Kinsman (Editor), J. Hopkins Univ., 154 pp.

Pritchard D.W. (1967). Observations of Circulation in Coastal Plain Estuaries. Chesapeake Bay Institute, The Hopkins University, p. 37-44

Rita P. Vasconcelos, Patrick Reis-Santos, Sofia Henriques, Susanne E. Tanner, Henrique N. Cabral, José L. Costa, Maria J. Costa. (2024) Chapter 4.7: River-Coast Connectivity, Estuarine Nursery Function and Coastal Fisheries, Treatise on Estuarine and Coastal Science (Second Edition), Academic Press, Pages 163-205,

Scully, M. E., Friedrichs, C., & Brubaker, J. (2005). Control of estuarine stratification and mixing by wind-induced straining of the estuarine density field. Estuaries, 28, 321–326. https://doi.org/10.1007/BF02693915

Shaha, D., Cho, YK. (2016). Salt Plug Formation Caused by Decreased River Discharge in a Multi-channel Estuary. *Sci Rep* 6, 27176

Solano J., Villalobos R. Regiones y Subregiones de Costa Rica. Instituto Meteorológico Nacional, Gestión de Desarrollo.

Temmerman, S., Meire, P., Bouman, T., Herman, P., Ysebaert, T., Vriend, H. (2013). *Ecosystem-based coastal defense in the face of global change*. Perspective, Nature 12859, DOI 10.1038

Valle-Levinson A. (2010). Contemporary Issues in Estuarine Physics. Cambridge University Press.

Valle-Levinson A., Schettini C., Truccolo E. (2014). Subtidal variability of exchange flows produced by river pulses, wind stress and fortnightly tides in a subtropical stratified estuary. Estuarine, Coastal and Shelf Science 221, p. 72-82

Valle-Levinson, A. (2022). *Introduction to Estuarine Hydrodynamics*, Cambridge: Cambridge University Press, DOI 10.1017

Viéytez A., Vásquez J., Palacios C., Chaquilla O., Calle C. R. (1983). Proyecto de Drenaje y Desarrollo Agrícola en la Cuenca del Rio Madre de Dios. Instituto Interamericano de Cooperación para la Agricultora (IICA), Instituto de Desarrollo Económico (IDE).

Weisstein, Eric W. (2022). Least Squares Fitting. From MathWorld--A Wolfram Resource. https://mathworld.wolfram.com/LeastSquaresFitting.html

Wetz, M., Yoskowitz, D. (2013). *An 'extreme' future for estuaries? Effects of extreme climatic events on estuarine water quality and ecology*. Marine Pollution Bulletine, Vol 69, p. 7-18 DOI 10.1016

Wolanski, E. & McLusky, D. S. (2011). Classification of the Estuarine Circulation. Treatise on Estuarine and Coastal Science 1st edn, Vol. 1 (ed. Valle-Levinson, A.) Ch. 1.05, 75–86